Concentration Dependence and Temperature Dependence of Hydrogen Tunneling in $Nb(OH)_x$

A. Magerl and A. J. Dianoux
Institut Laue-Langevin, 38042 Grenoble Cedex, France

H. Wipf
Institut für Festkörperphysik, Technische Hochschule Darmstadt, 6100 Darmstadt, West Germany

K. Neumaier
Walther-Meissner-Institut für Tieftemperaturforschung, 8046 Garching, West Germany

and

I. S. Anderson
University of Maryland, College Park, Maryland 20742
(Received 23 September 1985)

We have studied by neutron spectroscopy the concentration ($1.5\times10^{-4}\leq x\leq 1.1\times10^{-2}$) and temperature dependence ($0.5\ \mathrm{K}\leq T\leq 10\ \mathrm{K}$) of H tunneling in $Nb(OH)_x$. For $T<5$ K a narrow inelastic line is observed for $x=1.5\times10^{-4}$ which changes into a broad peak at higher concentrations. This shows that interactions between the defects lead to a distribution of both the asymmetry of the potentials and the matrix element. Between 5 and 10 K the data reveal a renormalization of the matrix element and an increased damping due to a Korringa-type coupling of the tunnel system with conduction electrons.

PACS numbers: 61.12.Ex, 61.40.+b, 63.20.Kr, 63.20.Mt

We report on the first spectroscopic measurements of both the concentration and temperature dependence of the tunnel splitting of the H vibrational ground state in $Nb(OH)_x$. The inelastic scattering at low temperatures shows the progressive influence of distortions with increasing defect concentration and a detailed analysis of the line shape allows us to distinguish between distortions of the tunnel system which lead to a purely energetic shift of the pocket states and distortions which cause a change of the matrix element. The evolution of the inelastic scattering with temperature is strongly indicative for the interaction of the tunnel systems with conduction electrons. This causes both different matrix elements for the superconducting and normal conducting states and a dynamical damping of the tunnel state, from which the electron-defect coupling constant can be determined.

Tunneling in $Nb(OH)_x$ has been observed by specific heat,[1-3] ultrasonic or inelastic studies,[4-9] and neutron-scattering[10,11] measurements. It is likely the best-known example for H tunneling in the solid state and it represents a unique model system with atomic transfer studies relevant for quantum diffusion theory.[12-14] A two-site model as commonly used to account for low-temperature anomalies in amorphous substances[15,16] has been proposed to describe the phenomenon. The energy difference E between the two lowest eigenstates of the H is then given by

$$E=(J_0^2+\epsilon^2)^{1/2}, \tag{1}$$

where J_0 is the matrix element and ϵ is an energetic shift between the two sites due to (elastic) defect-defect interaction. In view of the statistical spatial arrangement of the defects a distribution $Z(\epsilon)$ of Lorentzian shape[17] needs to be taken into account:

$$Z(\epsilon)=\pi^{-1}\Delta\epsilon/[(\Delta\epsilon)^2+\epsilon^2], \tag{2}$$

where $\Delta\epsilon$ is the average value for the energy shift. Similarly, a distribution $Z(J)$ with

$$Z(J)=\pi^{-1}\Delta J/[(\Delta J)^2+(J-J_0)^2] \tag{3}$$

can be assumed for the matrix element. The widths of both distributions will increase with increasing defect concentration when interactions become more important.[3]

Equation (4) is a generalization of the cross section for the inelastic scattering from a tunnel system [see Eq. (4) in Ref. 10], which includes the distribution functions for both the energy shift and the matrix element:

$$\frac{d^2\sigma}{d\Omega\, d(\hbar\omega)_{\mathrm{inel}}}=\frac{\sigma^{\mathrm{inc}}}{4\pi}\frac{k_f}{k_i}e^{-2W}\left(\frac{1}{2}-\frac{\sin Qd}{2Qd}\right)\int_{-\infty}^{\infty}dJ\,Z(J)\int_{-\infty}^{\infty}d\epsilon\,Z(\epsilon)\frac{J^2}{J^2+\epsilon^2}\frac{O(\hbar\omega)}{1+\exp(\hbar\omega/k_BT)} \tag{4a}$$

with

$$O(\hbar\omega)=\pi^{-1}\Gamma E^2/[(\hbar\omega)^2-E^2)^2+\Gamma\hbar\omega)^2], \tag{4b}$$

where σ^{inc} is the incoherent neutron-hydrogen cross section, $Q = k_i - k_f$, where k_f and k_i are the wave vectors of the neutron before and after the scattering process, e^{-2W} is the Debye-Waller factor, d is the distance between the pocket states, $k_B T$ gives the temperature, and $\hbar\omega$ is the energy transfer of the neutron.

The distributions in Eqs. (2) and (3) yield quite different scattering patterns. The inelastic intensity from systems with well-defined J_0 but with a distribution in ϵ has a steep onset at the energy J_0 and it extends to higher energy transfers (trailing edge). However, this scattering becomes rapidly reduced for increasing ϵ, while the elastic intensity from distorted potentials becomes correspondingly stronger. In contrast, the inelastic scattering from symmetric tunneling systems ($\Delta\epsilon = 0$) reflects the distribution $Z(J)$ and this results in a line broadening at both the low (leading edge) and high energy-transfer side (trailing edge) with respect to the peak position at J_0.

In Eq. (4) a dynamical coupling of the tunneling system to the environment is taken into account by the damped oscillator function $O(\hbar\omega)$ which is determined by the resonance frequency E and by the damping constant Γ. For small damping Γ the response function $O(\hbar\omega)$ becomes equivalent to δ functions located at positions $\pm E$.

The measurements were performed at the spectrometer IN6 at the Institute Laue-Langerin, Grenoble, with an elastic energy resolution of 0.055 meV (FWHM). Three sets of samples with defect concentrations $x = 1.1\times10^{-2}$, 2.2×10^{-3}, and 1.5×10^{-4} were used. Each was made out of three cylinders with a diameter of 10 to 12 mm and 60 mm high. More details will be given in a forthcoming paper.

The spectra observed between scattering angles of 60° and 120° were added together and a background from an empty cryostat run was subtracted. The data were fitted with the scattering law according to Eq. (4) for the inelastic scattering and a δ function for the elastic scattering, both convoluted with the measured resolution function. First, the dynamical damping was set equal to $\Gamma = 0$ to fit the spectra at 1.5 K for all three concentrations and the data were parametrized with respect to J_0, ΔJ, and $\Delta\epsilon$ and intensity parameters for elastic and inelastic scattering. Subsequently, the temperature dependence of the scattering measured for the sample with $x = 2.2\times10^{-3}$ was considered. Now ΔJ was held constant at the fitted value for 1.5 K, while Γ was introduced as a free parameter.

Figure 1 shows concentration dependence of the inelastic scattering measured at 1.5 K. Although the fits also included the positive-energy side, only the neutron energy-loss side is shown for increased clarity. The bold solid lines, the thin solid lines, and the dashed lines in Figs. 1 and 2 represent the fitted curve for the total scattering, the inelastic contribution, and the elastic scattering, respectively.

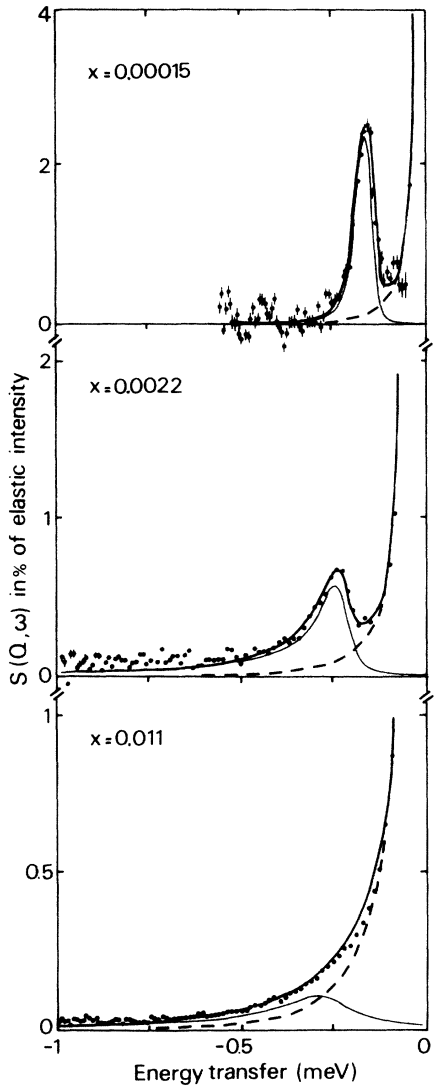

FIG. 1. Concentration dependence of the inelastic scattering measured at 1.5 K. See text for details. Note the different scales of the ordinates.

For $x = 1.5\times10^{-4}$ a well-defined inelastic peak is observed which reaches 2.5% of the elastic-peak intensity. As the best-fit values we obtain $\Delta\epsilon = 0.06 \pm 0.02$ meV, indicating that interactions are appreciable even at this low concentration, although the mean value for the asymmetry $\Delta\epsilon$ is smaller than the tunnel splitting $J_0 = 0.170 \pm 0.005$ meV. Within the accuracy of the data there is no indication of an intrinsic width of the leading edge which shows that all tunnel systems have the same matrix element ($\Delta J < 0.005$ meV).

For $x = 2.2\times10^{-3}$ the peak value of the inelastic scattering has decreased to 0.5% of the elastic peak intensity and the trailing edge has become much more pronounced. The matrix element has shifted to a higher value of $J_0 = 0.230 \pm 0.005$ meV in reasonable

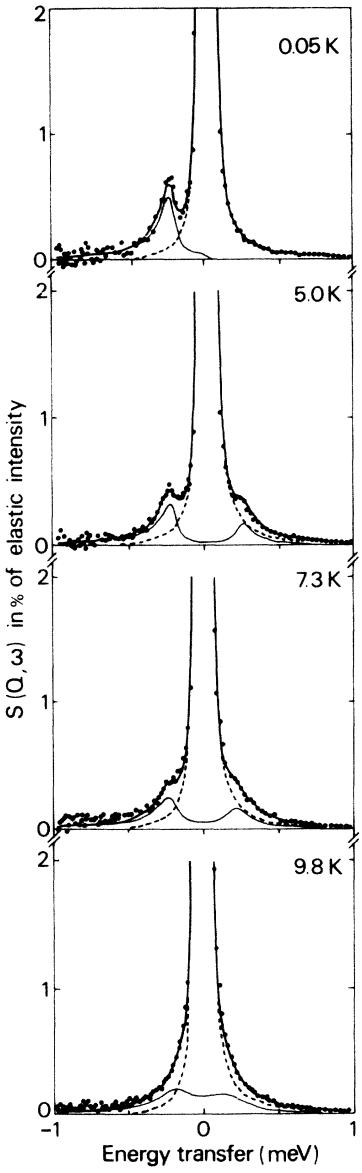

FIG. 2. Temperature dependence of the inelastic scattering for the sample with $x = 2.2 \times 10^{-3}$. See text for details.

agreement with earlier measurements on samples with similar concentration (0.21 ± 0.03 meV by neutron spectroscopy[11] and 0.19 ± 0.02 meV by specific heat[3]). A fit with Eq. (4) yields two problems. First, for $\Delta\epsilon >> J_0$, which is the case for this concentration, the peak shape changes only insignificantly with $\Delta\epsilon$, whereas the ratio between elastic and inelastic intensities remains sensitive to $\Delta\epsilon$. This has already been noted earlier[11] and will not be discussed further here. Second, we find some broadening of the leading edge of the inelastic peak and a distribution of the matrix element with $\Delta J = 0.015 \pm 0.008$ meV is required to describe its shape.

For $x = 1.1 \times 10^{-2}$ we observe both a further decrease of the inelastic peak intensity and a further

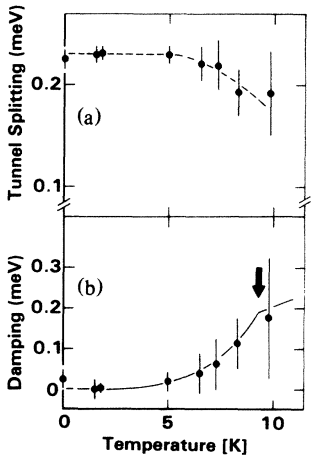

FIG. 3. Temperature dependence of (a) the tunnel splitting J_0 and of (b) damping Γ for the sample with $x = 2.2 \times 10^{-3}$. The arrow marks the superconducting transition temperature for pure Nb.

broadening of the leading edge. A fit yields again an increase of the tunnel splitting to $J_0 = 0.27$ meV and a distribution $\Delta J = 0.10$ meV. The fitted curve around -0.2 meV shows the leading edge somewhat broader than the experimental data, indicating that for this high concentration the Lorentzian distribution function in Eq. (3) no longer describes the details for $Z(J)$ accurately. Nevertheless, the essential feature is that both the largely broadened leading edge (dsitribution in J) and the weak inelastic intensity distributed over a wide energy range (distribution in ϵ) show the decisive influence of interactions between the tunnel systems which will eventually at even higher concentrations result in a glasslike behavior with a very broad distribution in J and ϵ.[18]

We now address the discussion of the temperature dependence of the inelastic scattering. Figure 2 demonstrates with some spectra the evolution between 0.5 and 9.8 K for the sample with $x = 2.2 \times 10^{-3}$. Up to 5 K, only the intensities for neutron energy loss and energy gain vary in accordance with the detailed balance factor. At higher temperatures, the line shape of the inelastic scattering changes and the separation from the elastic scattering becomes less pronounced. Figure 3 summarizes the results from the fits. Although the error bars become large for the higher temperatures the data above 5 K reveal an increase in the damping and a decrease of the energy splitting which likely is due to a renormalization of the matrix element J_0 by the conduction electrons.

To appreciate the strong damping of a tunnel motion already observable between 5 and 10 K, we note that Nb is a superconductor with a transition temperature of 9.2 K and the results in Fig. 3 suggest indeed a sensitivity of the tunnel system to the electronic state. This is also supported by recent ultrasonic measurements: A change in the damping pattern was observed

when a magnetic field was applied to a $Nb(NH)_x$ sample to destroy the superconducting state.[8]

If we assume a Korringa-type relaxation due to the interaction of the tunnel systems with the electrons, then the damping Γ for a BCS-type superconductor is given by[19]

$$\Gamma = (\pi/\hbar)(NV)^2 k_B T/\{1+\exp[\Delta(T)k_B T]\}, \quad (5)$$

where N is the electronic density of states per atom at the Fermi level, V is the matrix element for the scattering of electrons by the phonons, and $\Delta(T)$ is the superconducting gap energy. The solid line in Fig. 3(b) has been calculated from Eq. (5) with the zero-temperature gap energy of $\Delta(T=0)=1.5$ meV and with $NV=0.4$. The agreement with the measured temperature dependence of the damping Γ provides strong evidence that the observed relaxation originates indeed from the interactions with conduction electrons. Moreover, the value of $NV=0.4$ is similar to the value of the λ parameter ($\lambda=0.55$) for the electron-phonon interaction in Nb. This shows that the interactions of the electrons either with the phonons in Nb or with the delocalized H are of comparable strength.

In this context we propose that an activation energy of 1.8 meV derived from ultrasonic measurements[9] at temperatures $T<4$ K is not a feature of the level scheme of the tunnel system, but represents the superconducting gap energy measured via the electron-defect interaction. An extrapolation of the ultrasonic data into our temperature range by Eq. (5) reveals similar relaxation rates as observed in this work. This shows that the same tunnel systems were investigated in the ultrasonic measurements and in this investigation.

In summary, our neutron-spectroscopic study of H tunneling in $Nb(OH)_x$ shows that the inelastic intensity below 5 K is temperature independent except for the detailed balance factor. For $x=1.5\times10^{-4}$ the interactions between the defects are weak and all tunnel systems are practically equivalent. With higher concentrations the inelastic line becomes smeared out in energy and the inelastic peak height compared to the elastic peak is reduced as a result of increasing interactions between the defects. From a detailed analysis of the line shape the effect of these interactions on the distortions ϵ and on the matrix element J_0 have been separated. In the approach to the normal conducting state the data above 5 K reveal both a reduction of the matrix element and a strong intrinsic damping. The latter effect is attributed to a Korringa relaxation due to the interaction of the tunnel systems with conduction electrons. A value for the interaction strength has been obtained.

This work was in part supported by the Bundesministerium für Forschung und Technologie. We also acknowledge clarifying discussions with J. M. Rowe.

[1]G. J. Sellers, A. C. Anderson, and H. K. Birnbaum, Phys. Rev. B **10**, 2771 (1974).

[2]C. Morkel, H. Wipf, and K. Neumaier, Phys. Rev. Lett. **40**, 947 (1978).

[3]H. Wipf and K. Neumaier, Phys. Rev. Lett. **52**, 1308 (1984).

[4]E. L. Andronikashvili, V. A. Melik-Shakhnazarov, and I. A. Naskidashvili, J. Low Temp. Phys. **23**, 1 (1976).

[5]D. B. Poker, G. G. Setser, A. V. Granato, and H. K. Birnbaum, Z. Phys. Chem. **116**, 39 (1979).

[6]G. Canneli, R. Cantelli, and G. Vertechi, J. Less-Common Met. **88**, 335 (1982).

[7]G. Bellesa, J. Phys. (Paris), Lett. **44**, L387 (1983).

[8]J. L. Wang, G. Weiss, H. Wipf, and A. Magerl, in *Phonon Scattering in Condensed Matter,* edited by W. Eisenmenger, K. Lassmann, and S. Dottinger (Springer-Verlag, Berlin 1984), p. 401.

[9]D. B. Poker, G. G. Setser, A. V. Granto, and H. K. Birnbaum, Phys. Rev. B **29**, 622 (1984).

[10]H. Wipf, A. Magerl, S. M. Shapiro, S. K. Satija, and W. Thomlinson, Phys. Rev. Lett. **46**, 947 (1981).

[11]H. Wipf, K. Neumaier, A. Magerl, A. Heidemann, and W. Stirling, J. Less-Common Met. **101**, 317 (1984).

[12]M. I. Klinger, Phys. Rep. **94**, 183 (1983).

[13]M. Wagner, J. Phys. C **17**, 5289 (1984).

[14]J. Kondo, Physica (Amsterdam) **125B**, 279 (1984).

[15]P. W. Anderson, B. I. Halperin, and C. M. Varma, Philos. Mag. **25**, 1 (1972).

[16]W. A. Phillips, J. Low Temp. Phys. **7**, 351 (1972).

[17]A. M. Stoneham, Rev. Mod. Phys. **41**, 82 (1969).

[18]B. Fischer and M. W. Klein, Phys. Rev. Lett. **43**, 289 (1979); M. W. Klein, Phys. Rev. B **31**, 1114 (1985).

[19]See e.g., J. L. Black, in *Glassy Metals I,* edited by H. J. Guntherrodt and H. Beck, Topics in Applied Physics, Vol. 46 (Springer-Verlag, Berlin, 1981).